Decarbonization potential of the glass melting process via energy efficiency measures and fuel switching

Daniel Jost[a], Sara Kanzurova[a], Christiane Reinert[a], Niklas von der Aßen[a*]**

[a]Institute of Technical Thermodynamics, RWTH Aachen University, Schinkelstr. 8, 52062 Aachen, Germany, +49 241 80 95930, niklas.vonderassen@ltt.rwth-aachen.de, www.ltt.rwth-aachen.de

Abstract:

The production of glass is energy-intensive, with around 80 % of the energy required for the melting process. Hydrogen is a promising alternative fuel to decarbonize the glass melting process. Knowledge about the specific energy demand of the melting process is required for a quantitative assessment of the decarbonization potential of the glass melting process with hydrogen combustion. Currently, estimations for the specific energy demand for hydrogen-based glass production are missing an in-depth thermodynamic analysis.

The first contribution of this paper is to develop a model for the glass melting process with natural gas and hydrogen combustion based on ideal thermodynamics. Based on the process model, we then analyze the specific energy consumption, the direct CO_2 emissions, and the waste heat recovery potential for glass production. In addition, we use the well-established process of natural gas combustion with air as a benchmark. We compare the benchmark to the glass melting process based on alternative fuels: hydrogen/air, natural gas oxyfuel, and a hydrogen oxyfuel combustion.

In a case study for a flat glass furnace based on process parameters from the literature, we show that utilizing natural gas oxyfuel combustion for the glass melting process instead of natural gas/air combustion can already reduce the specific energy consumption by up to 17 %. The direct CO_2 emissions decrease up to 62 % compared to the benchmark process when combusting hydrogen as a result of avoiding combustion-related CO_2 emissions. In conclusion, our analysis allows to quantitatively assess the potential of a switch in fuel and oxidizer in the glass industry.

Keywords: thermodynamic analysis, hydrogen, oxyfuel, industrial decarbonization, glass industry, glass furnace

1 Introduction

The production of glass is energy-intensive, with around 80 % of the energy required for the melting process (Musgraves et al., 2019). The largest share of the energy demand is used for high-temperature heating in the endothermic glass melting process, typically provided by the combustion of natural gas. Unavoidable process emissions arise from the melting process due to the decomposition of CO_2 from carbonates in the raw materials. The rest of the direct CO_2 emissions arise from the natural gas combustion for the heat supply (Conradt, 2008). Due to increasing prices for CO_2 certificates and stricter limits for CO_2 emissions, decarbonizing the glass melting process is necessary, not only from an environmental, but also from an economic point of view.

In the literature, some decarbonization options for the glass melting process are deemed promising. The promising decarbonization options include the usage of cullet, waste heat recovery, electric boosting, fuel switching to hydrogen combustion, and oxyfuel combustion (Furszyfer Del Rio et al., 2022; Zier et al., 2021). Table 1 shows an overview of relevant literature that assesses the specific energy demand of the glass melting process, including these energy efficiency measures. All studied literature includes the specific energy demand of the glass melting process determined by thermodynamic analysis.

[**] Jungautor

[*] Corresponding author

Table 1 further covers whether the literature sources assess the direct CO_2 emissions, which is necessary to evaluate the decarbonization potential of the energy efficiency measures. Furthermore, we consider whether the studies conduct a thermodynamic analysis of the waste heat. An analysis of the waste heat is necessary to determine the best potential to further utilize the waste heat stream to reduce the specific energy demand and CO_2 emissions.

Table 1: Overview of selected decarbonization measures for the glass melting process in the literature.

	Usage of cullet	Waste heat		Electric boosting	Natural gas combustion		Hydrogen combustion		Direct CO_2 emissions
Source		Recovery	Exergy analysis		Air	Oxyfuel	Air	Oxyfuel	
(Sardeshpande et al., 2007)	x	x			x				
Conradt (2007)	x	x			x				
Conradt (2008)	x	x			x				
(Tapasa and Jitwatcharakomol, 2012)	x	x			x				
Lankhorst et al. (2014)	x	x		x	x				x
(Seo et al., 2020)	x	x		x	x				
Gärtner et al. (2021)	x	x		x	x	x		x	x
This study	**x**	**x**	**x**	**x**	**x**	**x**	**x**	**x**	**x**

Easy-to-exploit energy efficiency measures to reduce CO_2 emissions, for example using cullet and waste heat recovery, are already commercially used nowadays (Furszyfer Del Rio et al., 2022; Zier et al., 2021). In the first method, cullet with the same composition as the produced glass is melted with raw materials to reduce the energy demand as fewer raw materials have to be processed. Conradt (2008) proposes a method to derive the energy needed for the melting reaction based on the composition of the batch. The method considers the composition of raw materials and a specified fraction of the cullet to determine the so-called exploited heat. The exploited heat consists of the required heat for the batch-to-melt conversion and the sensible heat of the glass melt leaving the glass furnace.

Even though the required energy for the melting process decreases with an increasing fraction of the cullet, the maximum fraction of the cullet is limited for producing different types of glass to uphold the quality requirements (Furszyfer Del Rio et al., 2022; Musgraves et al., 2019).

Waste heat recovery (WHR) is another commercially-used energy efficiency measure. WHR utilizes the heat from the exhaust gas to preheat the oxidizer for fuel combustion to reduce the energy demand of the glass melting process (Furszyfer Del Rio et al., 2022; Musgraves et al., 2019). Conradt (2007) and Tapasa and Jitwatcharakomol (2012) propose a thermodynamic model based on heat balances to determine the glass melting process's specific energy demand including cullet and regenerative WHR. The model utilizes the thermodynamic calculations of the exploited heat presented by Conradt (2008) and extends the analysis by WHR. Conradt (2007) shows that configurations of specific pull rates and heat exploitation efficiencies can be determined for maximum production efficiency and sustainability.

Sardeshpande et al. (2007) present a thermodynamic model based on energy- and mass balances to derive the specific energy demand of the glass melting process. The results produced by the proposed model, including the one using cullet and WHR, are similar to that of produced by industrial furnaces. The authors show that an increase in the flue gas temperature by 50 °C after WHR increases the specific energy demand by 5 % indicating that WHR should aim for the technically lowest possible flue gas temperature.

The flue gas after the WHR typically consists of approximately 25-30 % of the furnace energy input (Furszyfer Del Rio et al., 2022). Additional waste heat utilization can further utilize the energy from the flue gas, e.g., for heat integration and electricity production with an Organic Rankine Cycle (Furszyfer Del Rio et al., 2022). The flue gases' composition and temperature must be known to optimally design additional WHR of the flue gas. As the quality of heat depends on the temperature, an analysis of the exergy for different fuels and oxidizers whilst varying flue gas temperature is necessary to determine the quantitative potential for additional waste heat utilization.

Electric boosting is another decarbonization option for the glass industry. In industrial applications, electric boosting is used as a supporting heat supply for the heat from fuel combustion. Nowadays, the percentage of electricity used to provide heat supply to the glass industry is approximately 17 % (Gärtner et al., 2021). Full direct electrification is discussed as one of the most promising decarbonization options because it allows the direct integration of low-carbon electricity. However, full direct electrification of the melting process is technically not feasible as yet for production volumes over 250 tons of glass per day (Furszyfer Del Rio et al., 2022; Zier et al., 2021). Seo et al. (2020) propose a physics-based model for a glass furnace, including electric boosting, to derive an optimal operation strategy for the demand response via dynamic optimization. The focus is on the optimal operation for two sources of energy supply: fuel combustion and electric boosting. The authors show using dynamic optimization that the demand-response-oriented electric boosting leads to a significant decrease in energy costs whilst being grid-serving for the electricity grid.

Oxyfuel combustion utilizes oxygen instead of ambient air as an oxidizer for the combustion. Utilization of oxygen can reduce the energy demand associated with heating up inert gases like nitrogen when the energy demand for the oxygen supply is lower than the energy savings (Gärtner et al., 2021; Musgraves et al., 2019; Zier et al., 2021). Lankhorst et al. (2014) present an energy balance model utilizing oxyfuel combustion, use of cullet, and WHR to assess the specific energy demand of the glass melting process and associated CO_2 emissions. A case study for an oxyfuel-fired glass furnace without using any cullet shows that the raw material composition strongly influences the specific energy demand and the direct CO_2 emissions. They conclude that depending on local prices for natural gas, electricity, oxygen, and raw material, a different batch composition can significantly reduce costs.

Hydrogen as an alternative fuel is discussed as a promising decarbonization option for the glass melting process. Hydrogen combustion avoids combustion-related CO_2 emissions leaving only process-related CO_2 emissions from calcination and CO_2 emissions for hydrogen supply (Zier et al., 2021). However, several studies raise concerns about hydrogen-based glass production. Major concerns include a lower radiation heat transfer of the flame from hydrogen combustion and a reduction in the furnace's operating lifespan due to higher combustion temperatures. The higher combustion temperature leads to a faster degradation of refractory materials. However, the studies highlight hydrogen-based glass production as a promising decarbonization option for the glass industry. (Furszyfer Del Rio et al., 2022; Iplik et al., 2022; Pisciotta et al., 2022; Zier et al., 2021)

Despite its immense potential for emission reduction, the specific energy demand of the glass melting process with hydrogen combustion is not well known. Gärtner et al. (2021) present a power-to-hydrogen concept for an oxyfuel glass melting process using a simulation approach. They propose a simulation model to assess the specific energy demand including the hydrogen supply chains. However, they only assume a static furnace efficiency for the glass furnace without a thermodynamic analysis of the furnace for different fuels. The focus of their study is on oxyfuel combustion where natural gas or hydrogen is used as the fuel. Natural gas and hydrogen combustion with air as the oxidizer is not covered in the study. Therefore, a thermodynamic analysis of the glass melting process with natural gas and hydrogen as the fuel and air or oxygen as the oxidizer is necessary to determine the fuel demand for a glass furnace.

Gärtner et al. (2021) show that for a hydrogen oxyfuel-fired glass furnace the specific energy demand including hydrogen production increases by 24 % compared to a natural gas oxyfuel-fired glass furnace. Furthermore, the authors show that the CO_2 emissions of the glass melting process utilizing hydrogen oxyfuel combustion only decrease when hydrogen and oxygen are produced using a low-carbon electricity source.

A comparative assessment of the specific energy demand of the glass melting process with alternative fuels and oxidizers is essential to quantify the potential for decarbonizing the glass melting process. Many studies analyze some specific options for the decarbonization at a time but an analysis considering all the mentioned alternatives could not be found in the literature. Therefore, we conduct an analysis of the glass melting process utilizing the commercially-used energy efficiency measures mentioned above. Hydrogen as alternative fuel and oxygen as alternative oxidizer is compared to the glass melting process based on natural gas and air. We consider all combinations of fuel and oxidizer in our study to quantitatively compare the potential for decarbonizing the glass melting process. For this purpose, we model the glass melting process with natural gas and hydrogen combustion based on ideal thermodynamics (Chapter 2). Our model includes four frequently discussed energy efficiency measures: cullet usage, WHR, electric boosting, and oxyfuel combustion. For a case study of a glass furnace for flat glass production (Section 3.1), we utilize the derived model to assess the specific energy demand (Section 3.2) and the direct CO_2 emissions (Section 3.3) of the melting process to evaluate the decarbonization potential of the hydrogen-based glass melting process. While upstream processes for hydrogen and oxygen supply should also be considered in a holistic analysis for energy demand and CO_2 emissions, we focus on the glass melting process to fill the gap of a detailed thermodynamic model and analysis thereof. The results of our gate-to-gate process approach can be considered as best-case potential with H_2 and O_2 being produced with renewables energy. Moreover, we conduct a thermodynamic exergy analysis to assess the potential for additional WHR (Section 3.4). We conclude our study by summarizing the key findings of the thermodynamic analysis of the hydrogen-based glass melting process (Chapter 4).

2 Model development

Understanding the thermodynamic behavior of the glass melting process is required to comprehend how the specific energy demand, the direct CO_2 emissions, and the WHR potential can be determined. Therefore, we present an overview of the process to show the system boundary of the melting process. We split the model description into four sections for a comprehensive discussion of energy and mass balances. All four sections are discussed separately and are as follows: the melting reaction (Section 2.1), the heat transfer (Section 2.2), the fuel combustion (Section 2.3), and the WHR (Section 2.4).

We model the glass melting process with natural gas and hydrogen combustion based on ideal thermodynamics. As shown in Figure 1, the system boundary contains the glass furnace, including the heat supply by fuel combustion, the melting reaction, WHR, electric boosting, and heat transfer. The model considers natural gas or hydrogen as a fuel and air or oxygen as an oxidizer for combustion. The process is described by mass and energy balances. We assume that there are no mass losses over the system boundary. The mass flow over the system boundary consists of the fuel, oxidizer, raw materials, cullet, and glass.

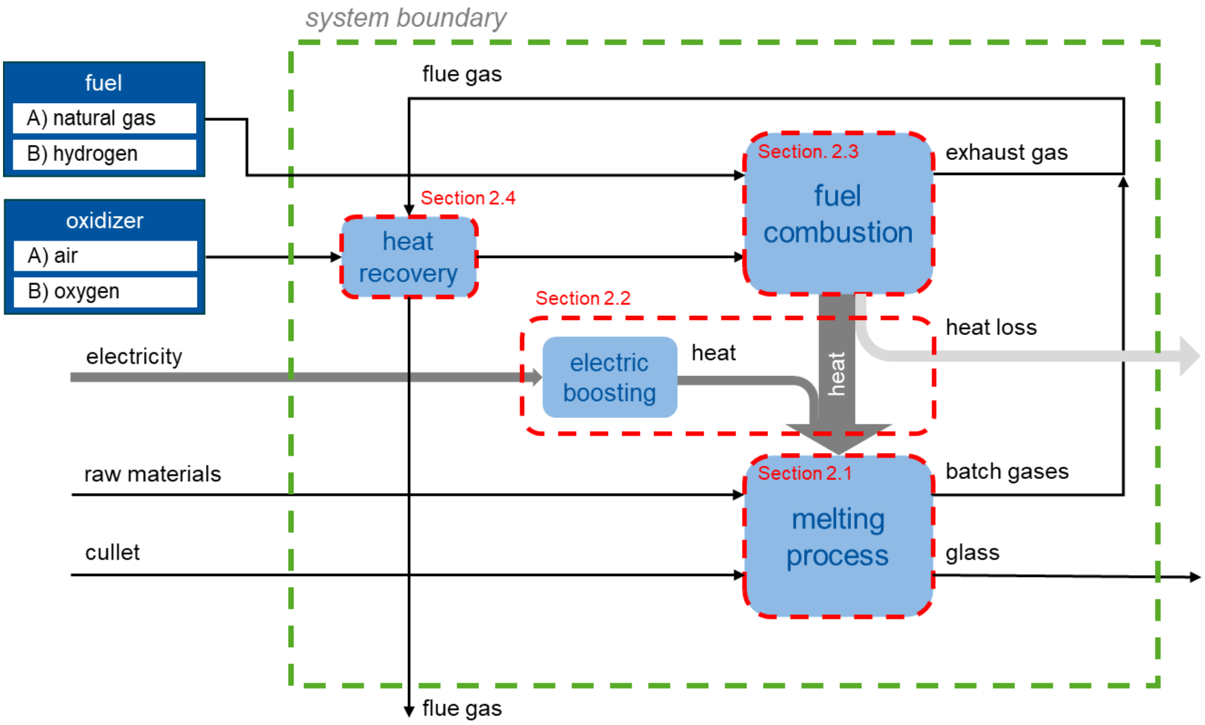

Figure 1: Schematic overview of the glass furnace model, including the heat supply by fuel combustion, the melting process, and four energy efficiency measures: usage of cullet, electric boosting, WHR, and oxyfuel combustion. The model considers natural gas or hydrogen as fuel and air or oxygen as an oxidizer for combustion. Fuel, oxidizer, electricity, raw materials, and cullet mark the inputs of the system boundary, while heat losses, glass, and flue gas are the system's outputs. The model is divided into four sections marked with the red dashed line.

We use the model to calculate the required amount of fuel, air, and electricity to produce one ton of glass and determine the potential for additional WHR based on exergy analysis of the flue gas. The exergy analysis allows a comparison of the waste heat at different flue gas temperatures.

As discussed before, the presented model considers four energy efficiency measures: use of cullet, WHR, electric boosting, and oxyfuel combustion. We utilize cullet, WHR, and electric boosting for all assessments in this study. We assess four fuel-combustion scenarios: natural gas/air combustion, hydrogen/air combustion, natural gas oxyfuel combustion, and hydrogen oxyfuel combustion. Natural gas/air combustion is used as the benchmark for our analysis as it is the most commonly used commercial glass melting process.

In the following sections, we describe the mathematical formulation of the model with mass and energy balances. We determine the mass and energy balances of the four outlined sub-processes of the glass melting process separately. The required heat for the melting reaction depends on the batch composition (Conradt, 2008; Musgraves et al., 2019). Therefore, the heat for the melting reaction is equal for all assessed scenarios.

We describe the thermodynamic relations of the melting process first. We show the mathematical formulation of the heat transfer from the fuel combustion and electric boosting for the glass melting process to determine the electricity demand and the heat that needs to be provided by combustion. Then, we determine the mass and energy balances for the fuel combustion. Lastly, we show the thermodynamic relations of the WHR. However, the energy balances of the fuel combustion and the WHR are dependent on each other, as the WHR utilizes the exhaust gas from combustion to preheat the air for the fuel combustion. Therefore, we determine the temperature of the preheated air in an iterative approach.

2.1 Glass melting reaction

The glass melting reaction describes the conversion of the batch consisting of raw materials and cullet into glass. Figure 2 shows the schematic system boundary of the glass melting reaction to determine the heat that is needed to convert the raw materials and cullet into glass and heat up the glass and batch gases. Furthermore, the amount of batch gases is determined.

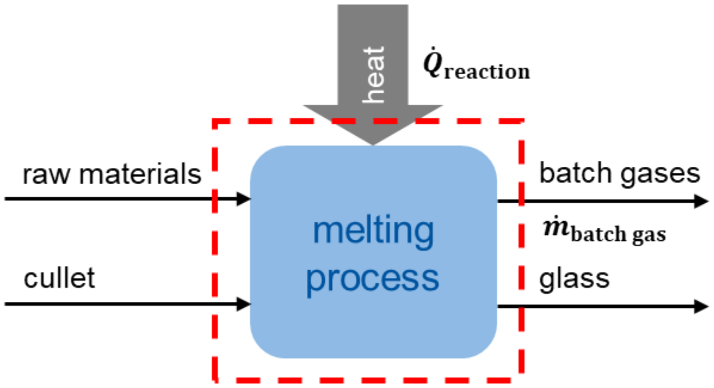

Figure 2: Schematic system boundary of the glass melting reaction to convert raw materials and cullet into glass. The heat for the process and the amount of batch gases need to be determined, while the other parameters are known.

As we assume that the batch contains moisture, the melting process requires additional energy for the heat of vaporization of water. We assume the use of cullet by internal recycling within the glass production process. Therefore, the cullet has the same composition as the produced glass. Equations (2.1) - (2.3) describe the mass balances for the melting reaction:

$$\dot{m}_{\text{batch}} = \dot{m}_{\text{glass}} + \dot{m}_{\text{batch gas}} \tag{2.1}$$

$$\dot{m}_{\text{batch}} = \dot{m}_{\text{raw material}} + \dot{\text{m}}_{\text{cullet}} + \dot{m}_{\text{H}_2\text{O}} \tag{2.2}$$

$$\dot{m}_{\text{cullet}} = y_{\text{cullet}} \cdot \dot{m}_{\text{glass}} \tag{2.3}$$

The batch gas mass flow $\dot{m}_{\text{batch gas}}$ contains CO_2 from the decomposition of carbonates within the raw materials and steam caused by moisture evaporation within the batch. y_{cullet} describes the fraction of cullet in relation to the produced glass. We consider a typical glass composition, consisting of lime (CaO), soda (NaO), silica sand (SiO_2), magnesia (MgO), alumina (Al_2O_3), and minor fractions of other materials (Tapasa and Jitwatcharakomol, 2012). Raw materials in this study are silica sand, soda ash ($NaCO_3$), dolomite, and alumina (Tapasa and Jitwatcharakomol, 2012). The main reactions of glass melting are the thermal decomposition of the mineral dolomite and the calcination of soda ash by reactive dissociation with silica sand. The calcination reaction results mainly in the formation of sodium silicates. Additionally, the raw materials of the soda-lime glass form different crystalline species (Musgraves et al., 2019; Verheijen, 2003). The different crystalline species of the raw materials are modelled in the glass reaction as reported by Tapasa and Jitwatcharakomol (2012). We assume that the batch composition allows a stoichiometric reaction to glass, consequently, a complete reaction to glass is assumed.

Equation (2.4) presents the energy balance for the heat for the glass melting reaction to calculate the heat demand for the melting reaction, including the decomposition of CO_2 from the raw materials and water evaporation in the batch:

$$\begin{aligned}\dot{Q}_{\text{reaction}} = \dot{m}_{\text{glass}} h_{\text{glass}}\left(T_{\text{glass}}\right) + \dot{m}_{\text{batch gas}} h_{\text{batch gas}}\left(T_{\text{batch gas}}\right) \\ - \dot{m}_{\text{batch}} h_{\text{batch}}(T_{\text{batch}})\end{aligned} \tag{2.4}$$

$\dot{Q}_{\text{reaction}}$ denotes the heat required for the endothermic melting reaction. $\dot{m}$ describes the mass flows of the glass, batch gases, and batch while $h(T)$ describes the enthalpy at a specific temperature T. Equation (2.4) can be expressed as the sum of thermal energy and the standard enthalpy of formation of the glass, batch gases, and batch of the melting reaction:

$$\dot{Q}_{\text{reaction}} = -\Delta\dot{H}_{\text{therm,reactants}} + \Delta\dot{H}_{\text{chem}} + \Delta\dot{H}_{\text{therm,products}} \tag{2.5}$$

$\Delta\dot{H}_{\text{therm,reactants}}$ and $\Delta\dot{H}_{\text{therm,products}}$ denote the thermal energy of the reactants (raw materials and cullet) and products (glass and batch gases) while $\Delta\dot{H}_{\text{chem}}$ describes the standard enthalpy of formation of the glass melting reaction. The batch and batch gases' thermal energy and formation enthalpies are modeled using ideal thermodynamics (Lucas, 2008). Due to chemical structure of glass, the standard enthalpy of formation for the glass cannot be determined using ideal thermodynamics. Therefore, in accordance to Conradt (2008) and Tapasa and Jitwatcharakomol (2012), the standard enthalpy of formation of glass is described by:

$$\Delta\dot{H}^{0,f}_{\text{glass}} = \sum_{k\in\text{raw materials}} \dot{n}_k \cdot \left(\Delta h^{f,0}_k + \Delta h^{\text{vit}}_k\right) \tag{2.6}$$

$\Delta\dot{H}^{0,f}_{\text{glass}}$ denotes the standard enthalpy of the formation of glass. The enthalpy is determined as a sum over the specific standard enthalpies of the formation $\Delta h^{f,0}_k$ and the specific vitrification enthalpy Δh^{vit}_k of each raw material k of the glass composition. These specific enthalpies are multiplied by the material flow rate $\dot{n}_k$ of each raw material. Furthermore, Conradt (2008) and Tapasa and Jitwatcharakomol (2012) determine the thermal energy of the glass at a temperature T according to Equations (2.7) - (2.10). In the literature, the reference point for determining the thermal energy of glass is set to 1400 °C (1673 K) (Conradt, 2008).

$$\Delta\dot{H}_{\text{therm,glass}} = \dot{H}_{T,\text{liq}}(T) - \Delta\dot{H}^{0,f}_{\text{glass}} \tag{2.7}$$

$$\dot{H}_{T,\text{liq}}(T) = \dot{H}_{1673\text{K,liq}} + \dot{C}_{P,\text{liq}} \cdot (T - 1673\text{ K}) \tag{2.8}$$

$$\dot{H}_{1673\text{K,liq}} = \sum_{k\in\text{raw materials}} \dot{n}_k \cdot h_{1673\text{K,liq},k} \tag{2.9}$$

$$\dot{C}_{P,\text{liq}} = \sum_{k\in\text{raw materials}} \dot{n}_k \cdot c_{P,\text{liq},k} \tag{2.10}$$

In Equation (2.7), the standard formation enthalpy of glass is the reference point for determining the thermal energy. $\dot{H}_{T,\text{liq}}(T)$ describes the enthalpy of the produced glass at a temperature T and is determined by Equation (2.8). There, $\dot{H}_{1673\text{K,liq}}$ denotes the enthalpy needed to heat the glass up to 1400 °C (1673 K). The enthalpy for the reference point of 1400 °C and the heat capacity flow $\dot{C}_{P,\text{liq}}$ of the glass composition are determined by Equations (2.9) and (2.10). $\dot{n}_k$ denotes the material flow rate while $h_{1673\text{K,liq},k}$ and $c_{P,\text{liq},k}$ describe the enthalpy for the reference point of 1400 °C and the heat capacity for each raw material k of the glass composition, respectively.

Utilizing the mass and energy balances, we determine the required energy for the glass reaction and the sensible heat of the glass and batch gases. We then utilize the calculated heat demand for the endothermic reaction and the energy demand for heating the components for the energy balance of the heat transfer.

2.2 Heat transfer

The heat demand from the fuel combustion and electric heating are determined in the heat transfer of the glass furnace. Figure 3 shows the schematic system boundary for the heat transfer in the glass furnace. The heat transfer covers the heat supply for the melting reaction from electric boosting and fuel combustion. The electric energy, the heat from fuel combustion, and the heat losses through the furnace walls are determined.

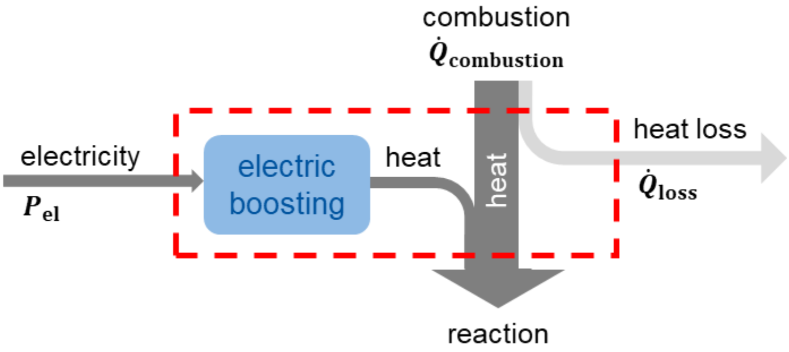

Figure 3: Schematic system boundary of the heat transfer in the glass furnace covering the heat for the melting reaction and the heat from electric boosting, fuel combustion, and losses over the furnace walls. The electric energy, the heat from combustion, and the heat losses through the furnace walls need to be determined, while the other parameters are known.

The heat demand for the melting reaction $\dot{Q}_{\mathrm{reaction}}$ is supplied with the heat supply from fuel combustion $\dot{Q}_{\mathrm{combustion}}$ and from electric boosting $\dot{Q}_{\mathrm{boosting}}$. The heating losses through the furnace walls is given as $\dot{Q}_{\mathrm{loss}}$ (Eq. (2.11)). The electric boosting utilizes conductive heating to supply heat directly into the glass melt. As the heating from electric boosting is limited, we assume the heat $\dot{Q}_{\mathrm{boosting}}$ to supply a constant fraction $\alpha_{\mathrm{boosting}}$ of the heat supply for the glass melting reaction $\dot{Q}_{\mathrm{reaction}}$ (Eq. (2.13)). We assume the heat losses $\dot{Q}_{\mathrm{loss}}$ as a fraction η_{furnace} of the heat provided by the fuel combustion (Eq. (2.14)).

$$\dot{Q}_{\mathrm{reaction}} = \dot{Q}_{\mathrm{combustion}} + \dot{Q}_{\mathrm{boosting}} - \dot{Q}_{\mathrm{loss}} \tag{2.11}$$

$$\dot{Q}_{\mathrm{boosting}} = \eta_{\mathrm{boosting}} \cdot P_{\mathrm{boosting}} \tag{2.12}$$

$$\dot{Q}_{\mathrm{boosting}} = \alpha_{\mathrm{boosting}} \cdot \dot{Q}_{\mathrm{reaction}} \tag{2.13}$$

$$\dot{Q}_{\mathrm{loss}} = \eta_{\mathrm{furnace}} \cdot \dot{Q}_{\mathrm{combustion}} \tag{2.14}$$

Utilizing Equations (2.11) - (2.14), we can calculate the required heat supply from the combustion with Equation (2.15):

$$\left(1 - \alpha_{\mathrm{boosting}}\right) \cdot \dot{Q}_{\mathrm{reaction}} = \left(1 - \eta_{\mathrm{furnace}}\right) \cdot \dot{Q}_{\mathrm{combustion}} \tag{2.15}$$

Heat demand is equal for all scenarios assessed in this study as the heat demand from fuel combustion solely depends on constant parameters and the heat for the melting reaction. The energy balances are used to determine the electric energy and heat from combustion that need to be supplied for the melting reaction.

2.3 Fuel combustion

The fuel combustion supplies the heat for the glass melting process. The schematic system boundary for the fuel combustion is shown in Figure 4. The amount of fuel, oxidizer, and resulting exhaust gas need to be determined whereas the process parameters are already known.

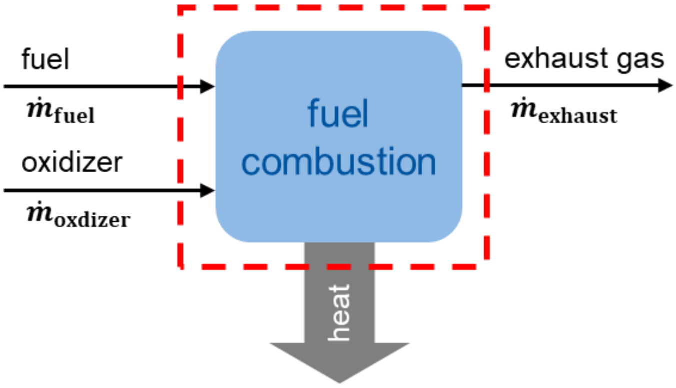

Figure 4: Schematic system boundary of the fuel combustion to supply heat for the melting reaction. The amount of fuel, oxidizer, and the resulting exhaust gas are determined whereas the process parameters are known.

The model considers preheated oxidizers from WHR to decrease the fuel demand and the heat losses within the exhaust gas. We assume a fixed exhaust gas temperature according to Tapasa and Jitwatcharakomol (2012) to ensure comparability of the different process configurations. We consider a slight over-stoichiometric combustion to reduce the formation of CO and NOx emissions (Gärtner et al., 2021). Therefore, we assume ideal and complete combustion of the fuels without the formation of CO and NOx as products. The exhaust gas consists of CO_2, H_2O, O_2, and N_2. For hydrogen combustion, the exhaust gas does not contain any CO_2, while for oxyfuel combustion, the exhaust gas does not contain N_2. Equation (2.16) describes the mass balances for the fuel combustion:

$$\dot{m}_{\text{fuel}} + \dot{m}_{\text{oxidizer}} = \dot{m}_{\text{exhaust}} \tag{2.16}$$

We can derive the combustion reactions for all assessed scenarios to determine the heat from fuel combustion. For brevity, we only denote the combustion reaction for the benchmark with natural gas/air combustion (Equation (2.17)), where λ denotes the excess air ratio:

$$\mathrm{CH_4} + \lambda \cdot 2\mathrm{O_2} + \lambda \cdot \frac{79}{21}\mathrm{N_2} \rightarrow \mathrm{CO_2} + 2\mathrm{H_2O} + (\lambda - 1) \cdot \mathrm{O_2} + \lambda \cdot \frac{79}{21}\mathrm{N_2} \tag{2.17}$$

Utilizing the combustion reactions, we derive the heat provided by the fuel combustion $\dot{Q}_{\text{combustion}}$ with an energy balance according to Equation (2.18):

$$\begin{aligned}\dot{Q}_{\text{combustion}} = {} & \dot{m}_{\text{fuel}} h_{\text{fuel}}(T_{\text{fuel}}) + \dot{m}_{\text{oxidizer}} h_{\text{oxidizer}}(T_{\text{oxidizer}}) \\ & - \dot{m}_{\text{exhaust}} h_{\text{exhaust}}(T_{\text{exhaust}})\end{aligned} \tag{2.18}$$

The fuel, oxidizer, and exhaust gas enthalpies are modeled using ideal thermodynamics (Lucas, 2008). As the temperature of the fuel and exhaust gas are known, we determine the temperature of the preheated oxidizer next. Therefore, we assess the mathematical formulation of the WHR.

2.4 Waste heat recovery

The WHR recovers the thermal energy of the batch gases and exhaust gas from the combustion to preheat the oxidizer for fuel combustion. Since the oxidizer is preheated, less fuel is required to provide the heat for the glass melting reaction. The schematic system boundary of the WHR is shown in Figure 5. The heat losses in the WHR, the exergy of the flue gas after the WHR, and the temperatures of the preheated oxidizer and the flue gas after WHR are determined, while the mass flows are known.

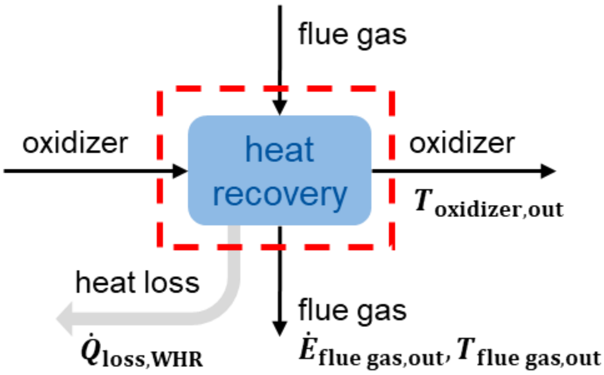

Figure 5: Schematic system boundary of the WHR to preheat oxidizer for the fuel combustion. The heat losses in the WHR, the exergy of the flue gas after the WHR, and the temperatures of the preheated oxidizer and the flue gas after WHR are determined, while the mass flows are known.

Within the glass industry, WHR typically utilizes regenerators for glass furnaces with a high production volume (Furszyfer Del Rio et al., 2022). We assume that there are no mass losses within the regenerator. We utilize two mass balances to describe the WHR, one balance for the exhaust gas stream (Eq. (2.19)) and one balance for the oxidizer stream (Eq (2.20)):

$$\dot{m}_{\text{flue gas}} = \dot{m}_{\text{exhaust}} + \dot{m}_{\text{batch gas}} \tag{2.19}$$

$$\dot{m}_{\text{flue gas,in}} = \dot{m}_{\text{flue gas,out}} = \dot{m}_{\text{flue gas}} \tag{2.20}$$

$$\dot{m}_{\text{oxidizer,in}} = \dot{m}_{\text{oxidizer,out}} \tag{2.21}$$

We determine the heat $\dot{Q}_{\text{WHR}}$ that can be utilized for WHR with an energy balance, according to Equation (2.22). We assume the heat losses $\dot{Q}_{\text{loss,WHR}}$ over the walls of the regenerator as a share η_{WHR} of the thermal energy of the hot flue gas stream (Eq. (2.23)). It is desirable to increase the thermal energy that can be utilized for WHR as this leads to an increased temperature of the preheated oxidizer. However, the minimal flue gas temperature after the WHR is constrained (Furszyfer Del Rio et al., 2022). Therefore, we fix the minimal flue gas temperature after the WHR to a literature value for all assessed scenarios (Sardeshpande et al., 2007; Tapasa and Jitwatcharakomol, 2012). Fixing the minimal flue gas temperature after the WHR at similar process conditions ensures the results are comparable for different scenarios. When the heat from the flue gas is higher than the heat required to preheat the air, we allow a higher temperature for the flue gas after the WHR.

$$\dot{Q}_{\text{WHR}} = \dot{m}_{\text{flue gas}} h_{\text{flue gas,in}}\left(T_{\text{flue gas,in}}\right) - \dot{m}_{\text{flue gas}} h_{\text{flue gas}}\left(T_{\text{flue gas}}\right) - \dot{Q}_{\text{WHR,loss}} \tag{2.22}$$

$$\dot{Q}_{\text{loss,WHR}} = \eta_{\text{WHR}} \cdot \dot{m}_{\text{flue gas}} h_{\text{flue gas,in}}\left(T_{\text{flue gas,in}}\right) \tag{2.23}$$

As we determine the potential of decarbonization options for the glass melting process, achieving a maximal temperature of the preheated oxidizer is desirable for a best-case analysis. Heat loss through the regenerator walls decreases the temperature of the flue gas that can be used to preheat the oxidizer. Therefore, the flue gas temperature $T'_{\text{flue gas,in}}$ is determined taking in account the heat loss in the energy balance shown by Equations (2.24) and (2.25):

$$\dot{Q}_{\text{WHR}} = \dot{m}_{\text{flue gas}} h_{\text{flue gas,in}}\left(T_{\text{flue gas,in}}{}'\right) - \dot{m}_{\text{flue gas}} h_{\text{flue gas,out}}\left(T_{\text{flue gas,out}}\right) \tag{2.24}$$

$$\dot{m}_{\text{flue gas}} h_{\text{flue gas,in}}\left(T_{\text{flue gas,in}}{}'\right) = \dot{m}_{\text{flue gas,in}} h_{\text{flue gas,in}}\left(T_{\text{flue gas,in}}\right) - \dot{Q}_{\text{loss,WHR}} \tag{2.25}$$

With the calculated heat that the WHR can utilize, we calculate the temperature of the preheated air by an energy balance given by Equation (2.26). The flue gas temperature $T'_{\mathrm{flue\ gas,in}}$ constrains the temperature of the preheated air $T_{\mathrm{oxidizer,out}}$ (Eq. (2.27))

$$\dot{Q}_{\mathrm{WHR}} = \dot{m}_{\mathrm{oxidizer,out}} h_{\mathrm{oxidizer,out}}\left(T_{\mathrm{oxidizer,out}}\right) - \dot{m}_{\mathrm{oxidizer,in}} h_{\mathrm{oxidizer,in}}\left(T_{\mathrm{oxidizer,in}}\right) \tag{2.26}$$

$$T'_{\mathrm{flue\ gas,in}} \geq T_{\mathrm{oxidizer,out}} \tag{2.27}$$

The flue gases' temperature and mass flow vary for the assessed scenarios with different fuels and oxidizers. Therefore, the thermal energy of the flue gas is not comparable for an analysis of the WHR potential. An analysis of the exergy is required to assess the WHR potential as the exergy takes the temperature level of the heat into account. The exergy $\dot{E}_{\mathrm{flue\ gas}}$ of the heat of the flue gas stream at the flue gas temperature $T_{\mathrm{flue\ gas,out}}$ is determined by Equation (2.28) where T_{u} is the ambient temperature as is taken as the reference temperature and $s(T)$ denotes the entropy of the flue gas at a temperature T:

$$\begin{aligned}\dot{E}_{\mathrm{flue\ gas}} = \dot{m}_{\mathrm{flue\ gas}} \Big[& \Big(h_{\mathrm{flue\ gas}}\left(T_{\mathrm{flue\ gas,out}}\right) - h_{\mathrm{flue\ gas}}(T_{\mathrm{u}})\Big) \\ & - T_{\mathrm{u}} \Big(s_{\mathrm{flue\ gas}}\left(T_{\mathrm{flue\ gas,out}}\right) - s_{\mathrm{flue\ gas}}(T_{\mathrm{u}})\Big)\Big]\end{aligned} \tag{2.28}$$

The complete thermodynamic modeling of the glass melting process now allows a best-case comparison of the different alternative fuels and oxidizers for a quantitative analysis of the decarbonization potential.

3 Results

We utilize the derived model to analyze the specific energy demand, the direct CO_2 emissions from combustion and melting reaction, and the exergy of the waste heat to assess the potential for additional WHR. First, we present the case study and process parameters used to obtain the results (Section 3.1). The specific energy demand, consisting of a fuel and an electricity demand, is determined for the glass melting process to produce one ton of glass (Section 3.2). The direct CO_2 emissions are determined and consist of the combustion-related and process-related emissions from the fuel combustion and the glass reaction (Section 3.3). Lastly, we assess the exergy of the heat from the flue gas to determine the potential for additional WHR (Section 3.4).

3.1 Case Study

As a case study, we generate the decarbonization potential of using different fuels to produce flat glass. The glass composition and the material data of the raw materials and glass are taken from the literature (Conradt, 2008; Tapasa and Jitwatcharakomol, 2012). We make several assumptions to simplify the determination of the specific energy demand, the direct CO_2 emissions, and the exergy of the flue gas. For simplicity, we assume that natural gas contains solely methane and air is an ideal gas consisting of only nitrogen and oxygen. The fuel, oxidizer, raw materials, and cullet are fed into the process at ambient temperature as the thermal energy of the streams can be neglected in the energy balances then. The material data for the gaseous streams are taken from the literature (Thomas C. Allison, 2013). Table 2 shows the process parameters from the literature used for the case study.

To assess the quantitative potential of alternative fuels and oxidizers, we evaluate four scenarios that differ in the choice of fuel and oxidizer:

- Natural gas/air combustion
- Hydrogen/air combustion
- Natural gas oxyfuel combustion
- Hydrogen oxyfuel combustion.

Table 2: Process parameters used in this study.

parameter	value	unit	source
ambient temperature	25	°C	
temperature air input	25	°C	
temperature fuel	25	°C	
temperature raw materials	25	°C	
temperature cullet	25	°C	
temperature glass output	1359	°C	(Tapasa and Jitwatcharakomol, 2012)
temperature exhaust gas	1396	°C	(Tapasa and Jitwatcharakomol, 2012)
minimal temperature flue gas	540	°C	(Tapasa and Jitwatcharakomol, 2012)
moisture batch	4	%	(Sardeshpande et al., 2007)
fraction of cullet	40	%	(Sardeshpande et al., 2007)
share of electric boosting	8	%	(Seo et al., 2020)
heat losses melting process	16.5	%	(Sardeshpande et al., 2007)
heat losses WHR	4.9	%	(Sardeshpande et al., 2007)
excess air ratio	1.05	-	(Gärtner et al., 2021)

3.2 Specific energy demand

We assess the specific energy demand of the glass melting process to produce one ton of glass. The energy demand consists of the electricity demand for the electric boosting and the fuel demand for the combustion. As shown in Figure 6, the specific energy demand decreases relative to the benchmark when switching the fuel or the oxidizer.

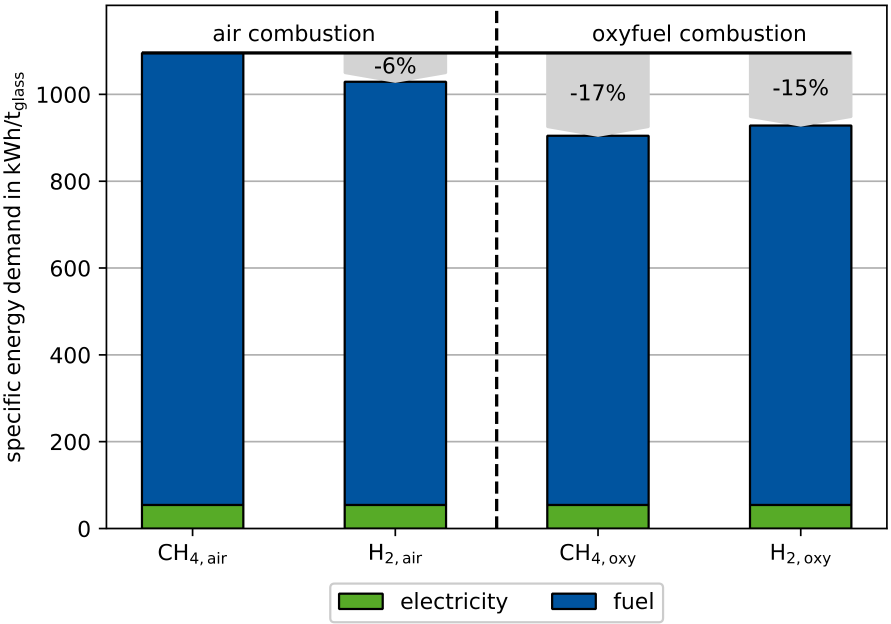

Figure 6: Specific energy demand in kWh to produce one ton of glass utilizing cullet, electric boosting, and WHR as energy efficiency measures. The electricity demand is shown in green, while the fuel demand is shown in blue. The first two bars show the specific energy demand with air as the oxidizer, while the other two bars show the specific energy demand for oxyfuel combustion. The arrows indicate the relative reduction of the specific energy demand for the glass melting process.

As we model the electric boosting as a fraction of the heat demand for the glass melting reaction, the electricity demand is equal for all assessed scenarios. In the benchmark with natural gas/air combustion, 51.7 kWh of electricity for electric boosting and 1.04 MWh of natural gas for fuel combustion are needed to produce one ton of glass. If the fuel is switched to hydrogen it reduces the fuel demand by 6.3 % to 0.97 MWh fuel per ton of glass. The total specific energy demand decreases by 6.0 % for hydrogen/air combustion. Utilizing oxyfuel combustion reduces the specific energy demand by 17 % for natural gas and by 15 % for hydrogen combustion. Therefore, changing the oxidizer to oxygen is more favorable than a fuel switch towards hydrogen without changing the oxidizer when the specific energy demand is considered. Of course, oxygen supply requires energy as well. However, if hydrogen is produced via electrolysis the right amount of (typically unused) oxygen is co-produced and available for oxyfuel combustion.

3.3 Direct CO_2 emissions

We assess the direct CO_2 emissions from the glass melting process. As we assess only the potential to mitigate direct emissions, we neglect emissions from feedstock, fuel, oxygen, and electricity supply chains. Future studies should consider supply chains for a holistic analysis of decarbonization options for the glass melting process. Nevertheless, our results give a best-case potential for CO_2 emission reduction if fuels and oxygen are produced with renewable energy. Figure 7 shows the direct CO_2 emissions per ton of glass.

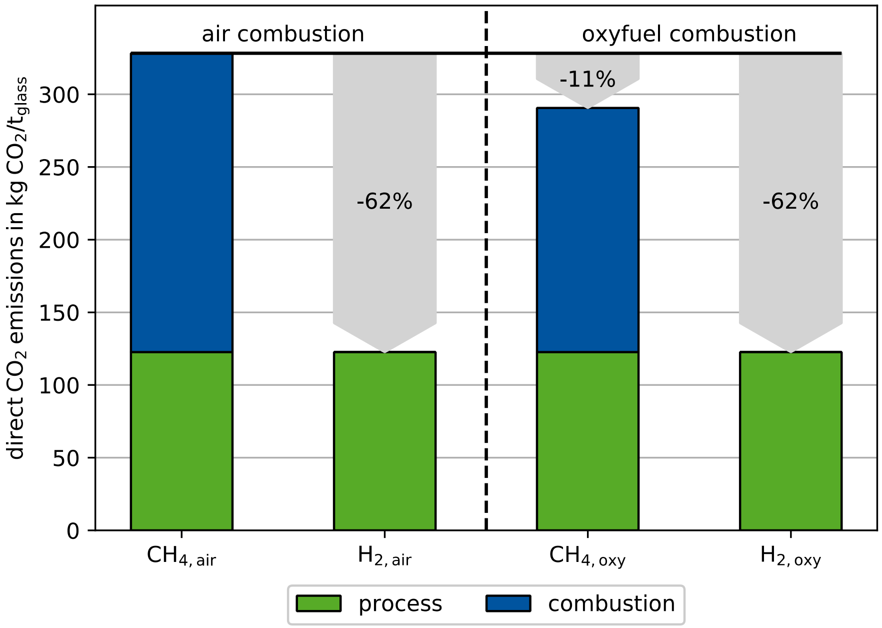

Figure 7: Direct CO_2 emissions for the glass melting process in kg to produce one ton of glass. The first two bars show the direct CO_2 emissions from combustion with air as the oxidizer, while the other two bars show the direct CO_2 emissions for oxyfuel combustion. The arrows indicate the relative reduction of the direct CO_2 emissions for the glass melting process.

Results differentiate between process-related and combustion-related direct CO_2 emissions. As the process emissions depend on the batch composition and not the fuel type, the same process emissions occur for all scenarios (Lankhorst et al., 2014). The process emissions are 122.6 kg CO_2 per ton of glass produced. Hydrogen combustion avoids combustion-related CO_2 emissions, leaving only process-related direct CO_2 emissions. For the benchmark scenario, combustion-related emissions account for 205.6 kg CO_2 per ton of glass. The combustion-related emissions decrease by 18.3 % to 167.9 kg CO_2 per ton of glass for natural gas oxyfuel combustion. The overall direct CO_2 emissions for natural gas oxyfuel combustion consisting of process-related and combustion-related emissions decrease by 11.46 % by avoiding the sensible heat required for heating the inert nitrogen in the air. When using hydrogen as the fuel for combustion, the remaining direct CO_2 emissions consist of process-related emissions only. The emissions decrease by 62 %, down to 122.6 kg CO_2 per ton of glass. Therefore, a fuel switch from natural gas to hydrogen is significantly favorable to reduce direct CO_2 emissions for glass production significantly.

3.4 Exergy of the waste heat

We assess the exergy of the flue gas stream from the glass melting process per ton of glass. Exergy analysis is required as the resulting temperature of the flue gas changes significantly within the four scenarios. The exergy analysis considers the temperature of the flue gas to make the different scenarios comparable. The exergy is determined as shown in Section 2.4. Figure 8 shows the results of the assessment of the thermal energy and exergy of the flue gas from the glass furnace.

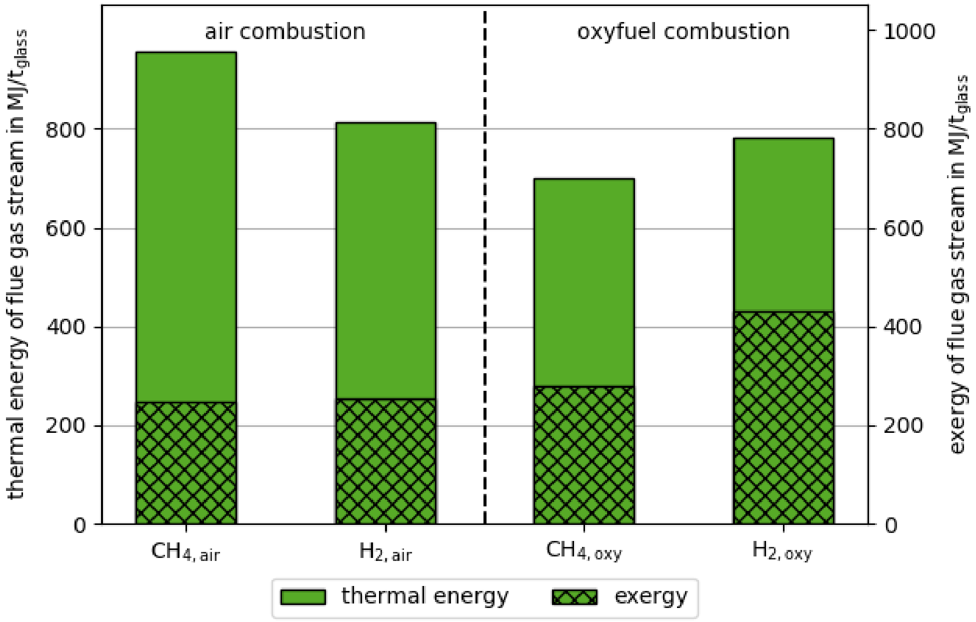

Figure 8: Assessment of the thermal energy and exergy of the flue gas of the glass melting process. The heat is shown in green, while the exergy is marked hatched as a share of the thermal energy. The first two bars show the thermal energy and exergy for fuel combustion with air as the oxidizer, while the other two bars show the thermal energy and exergy for oxyfuel combustion.

The flue gas stream for the benchmark process has an exergy of 407.8 MJ per ton of glass. The flue gas temperature is equal to the minimal flue gas temperature of 540 °C for the benchmark process. The exergy of the flue gas increases by 12.5 % for the melting process with natural gas oxyfuel combustion, while the temperature of the flue gas increases to 1022 °C. In comparison, the exergy increases by 2 % for the melting process with hydrogen/air combustion with the flue gas temperature remaining at 540 °C. For the process with hydrogen oxyfuel combustion, the exergy of the flue gas increases by 74.3 % to 431.7 MJ per ton of glass. The rise in the exergy is a result of the significant increase in the temperature of flue gas for hydrogen oxyfuel combustion. The flue gas temperature for hydrogen oxyfuel combustion increases to 1102 °C due to a high thermal energy of the flue gas.

The process with hydrogen oxyfuel combustion shows a significantly improved potential compared to the benchmark for utilizing the flue gas waste heat. Therefore, the glass melting with oxyfuel combustion is favorable as an alternative process for glass melting. The highest potential for additional WHR offers the glass melting process with hydrogen oxyfuel combustion.

4 Conclusion

In this work, we develop a thermodynamic model based on mass and energy balances for the glass melting process. We consider four energy efficiency measures in the model: use of cullet, WHR, electric boosting, and oxyfuel combustion. We consider natural gas or hydrogen as fuel and air or oxygen an oxidizer for fuel combustion. The process with natural gas/air combustion marks the benchmark for the analysis. The specific energy demand, the direct CO_2 emissions, and the exergy of the flue gas are determined to assess the different process configurations of fuel and oxidizer.

We present a case study for a flat glass furnace based on the literature. The specific energy demand decreases by 17 % compared to the benchmark when using natural gas oxyfuel combustion. When utilizing hydrogen air and oxyfuel combustion the specific energy demand decreases by 7 % and 15 %, respectively. Therefore, changing the oxidizer to oxygen is more favorable than a fuel switch towards hydrogen without changing the oxidizer when energy demand is being considered. With hydrogen combustion, the direct CO_2 emissions are reduced by 62 % where combustion-related CO_2 emissions are avoided. With hydrogen combustion, the remaining emissions are solely the process emissions from the glass melting reaction. Therefore, the hydrogen-based glass melting process is more favorable than the benchmark for reducing direct CO_2 emissions. The glass melting process with hydrogen oxyfuel combustion is more favorable than the benchmark as it offers the highest potential for additional waste heat utilization.

The exergy of the flue gas increases by 12.5 % for the glass melting process with natural gas oxyfuel combustion whereas the exergy of the flue gas increases by 74.3 % with hydrogen oxyfuel combustion. The increase in the exergy of the flue gas is due to the higher temperature of the flue gas. Further research regarding additional WHR is desirable to determine optimal technologies to maximize CO_2 mitigation of the glass melting process.

5 References

Conradt, R., 2007. Production efficiency, environmental sustainability, and glass quality – a thermodynamic optimization of three conflicting objectives. Glass Technology - European Journal of Glass Science and Technology Part A, 235–241.

Conradt, R., 2008. The industrial glass-melting process, in: The SGTE Casebook. Elsevier, pp. 282–303.

Furszyfer Del Rio, D.D., Sovacool, B.K., Foley, A.M., Griffiths, S., Bazilian, M., Kim, J., Rooney, D., 2022. Decarbonizing the glass industry: A critical and systematic review of developments, sociotechnical systems and policy options. Renewable and Sustainable Energy Reviews 155, 111885.

Gärtner, S., Rank, D., Heberl, M., Gaderer, M., Dawoud, B., Haumer, A., Sterner, M., 2021. Simulation and Techno-Economic Analysis of a Power-to-Hydrogen Process for Oxyfuel Glass Melting. Energies 14, 8603.

Iplik, E., Adendorff, M., Muren, D., 2022. Hydrogen Oxyfuel Combustion for Energy-Intensive Industries. Clean Energy Technologies 2022.

Lankhorst, A., Thielen, L., van der Dennen, J., del Hoyo Arroyo, M., 2014. Application of an Energy Balance Model for Improving the Energy Efficiency of Glass Melting Furnaces, in: Sundaram, S.K. (Ed.), 74th Conference on Glass Problems. John Wiley & Sons, Inc, Hoboken, NJ, USA, pp. 51–68.

Lucas, K., 2008. Thermodynamik: Die Grundgesetze der Energie- und Stoffumwandlungen, 7th ed. Springer, Berlin, Heidelberg, Online-Ressource.

Musgraves, J.D., Hu, J., Calvez, L., 2019. Springer Handbook of Glass. Springer International Publishing, Cham, 1851 pp.

Pisciotta, M., Pilorgé, H., Feldmann, J., Jacobson, R., Davids, J., Swett, S., Sasso, Z., Wilcox, J., 2022. Current state of industrial heating and opportunities for decarbonization. Progress in Energy and Combustion Science 91, 100982.

Sardeshpande, V., Gaitonde, U.N., Banerjee, R., 2007. Model based energy benchmarking for glass furnace. Energy Conversion and Management 48, 2718–2738.

Seo, K., Edgar, T.F., Baldea, M., 2020. Optimal demand response operation of electric boosting glass furnaces. Applied Energy 269, 115077.

Tapasa, K., Jitwatcharakomol, T., 2012. Thermodynamic calculation of exploited heat used in glass melting furnace. Procedia Engineering 32, 969–975.

Thomas C. Allison, 2013. NIST-JANAF Thermochemical Tables - SRD 13.

Verheijen, O.S., 2003. Thermal and chemical behavior of glass forming batches, 224 pp.

Zier, M., Stenzel, P., Kotzur, L., Stolten, D., 2021. A review of decarbonization options for the glass industry. Energy Conversion and Management: X 10, 100083.